Eur. Phys. J. C 11, 69–78 (1999)
Digital Object Identifier (DOI) 10.1007/s100529900148

THE EUROPEAN PHYSICAL JOURNAL C

Quasi-elastic pn scattering in ^{6}LiD and ^{6}LiH targets from 1.1 to 2.4 GeV

A. de Lesquen[1], C.E. Allgower[2], J. Ball[1,3], M. Beddo[2,a], J. Bystrický[1], M. Combet[1,3], Ph. Demierre[4], G. Durand[1], J.-M. Fontaine[1,3], D. Grosnick[2,b], R. Hess[4,†], Z. Janout[5,c], Z.F. Janout[4,d], V.A. Kalinnikov[5], T.E. Kasprzyk[3], B.A. Khachaturov[5], R. Kunne[3,e], F.Lehar[1], D. Lopiano[2,f], V.N. Matafonov[5], I.L. Pisarev[5], A.A. Popov[5], A.N. Prokofiev[6], D. Rapin[4], J.-L. Sans[3,g], H.M. Spinka[2], Yu.A. Usov[5], V.V. Vikhrov[6], B. Vuaridel[4], A.A. Zhdanov[6]

[1] DAPNIA, CEA/Saclay, 91191 Gif-sur-Yvette Cedex, France
[2] Argonne National Laboratory, HEP Division, 9700 South Cass Avenue, Argonne, IL 60439, USA
[3] Laboratoire National SATURNE, CNRS/IN2P3 and CEA/DSM, CEA/Saclay, 91191 Gif-sur-Yvette Cedex, France
[4] DPNC, University of Geneva, 24 quai Ernest-Ansermet, 1211 Geneva 4, Switzerland
[5] Laboratory of Nuclear Problems, JINR, 141980 Dubna, Moscow Region, Russia
[6] Petersburg Nuclear Physics Institute, 188350 Gatchina, Russia

Received: 19 April 1999 / Published online: 28 September 1999

Abstract. A polarized proton beam from SATURNE II, the Saclay polarized targets with ^{6}Li compounds, and an unpolarized CH_2 target were used to measure spin-dependent observables for protons scattered on bound nucleons. The beam and target polarizations were oriented vertically. The analyzing power A_{oono} and the depolarization D_{nono} were determined at seven energies between 1.1 and 2.4 GeV. The spin correlation parameter A_{oonn} was measured at only 1.1 and 1.6 GeV. Measurements with the CH_2 target at 1.1 GeV provided A_{oono} data for scattering of polarized protons on neutrons in carbon. The quasi-elastic observables are compared with previous elastic scattering measurements and at 1.1 GeV with predictions of phase shift analyses.

1 Introduction

The aim of the measurements presented in this paper is to compare the elastic and quasi-elastic spin-dependent observables in order to extend the energy region of pn data. The pn and the pp data were recorded simultaneously. The pp part of the experiment was described in the preceding paper [1]. The new polarizable target materials ^{6}LiD and ^{6}LiH were successively used, and scattering of polarized protons on bound neutrons was studied. The beam polarization $\vec{P}_{\mathrm{B}}$ and target polarization $\vec{P}_{\mathrm{T}}$ were oriented vertically. An unpolarized CH_2 reference target was positioned behind the main target, and scattering of polarized protons on nucleons in carbon was measured.

The beam kinetic energy of 1.1 GeV is close to the highest free polarized neutron beam energy at SATURNE II. Above 0.8 GeV, spin-dependent observables measured at this accelerator allowed us to perform phase shift analyses (PSA) [2,3] and a direct reconstruction of the scattering matrix [3]. In the present experiment, the pn analyzing power A_{oono} and the depolarization D_{nono} were measured between 1.1 and 2.4 GeV, whereas the spin correlation parameter A_{oonn} was obtained at only 1.1 and 1.6 GeV.

The determination of the observables from the recorded data has been discussed in the preceding paper [1] and will not be repeated, nor will the description of the proton beam extraction, polarimeters, or targets. In Sect. 2, we review the existing database for the relevant np and pn observables between 1.0 and 2.7 GeV. In Sect. 3, the experimental setup and the data analysis are briefly described. The results are presented in Sect. 4. They are compared with existing data where possible. At 1.095 GeV, the data are compared with the energy-dependent Virginia Polytechnic Institute PSA (VPI-PSA) [2] and with the Saclay-Geneva PSA (SG-PSA) at fixed energy [3].

Throughout the paper, we use the nucleon–nucleon formalism and the four-index observable notation given in [4]. The subscripts of any observable X_{srbt} refer to the polarization states of the scattered, recoil, beam, and target

Present address:
[a] Data Ventures LLC, Los Alamos, NM 87544, USA
[b] Department of Physics and Astronomy, Valparaiso University, Valparaiso, IN 46383, USA
[c] Faculty of Nuclear Sciences and Physical Engineering, Czech Technical University, Břehová 7, 11519 Prague 1, Czech Republic
[d] Computing Center of the Czech Technical University, Zikova 4, 16635 Prague 6, Czech Republic
[e] Institut de Physique Nucléaire IN2P3, 91400 Orsay, France
[f] 101 Aroyo del Mar Court, Aptos, CA 95003, USA
[g] Centrale Themis, 66121 Targasonne, France
[†] Deceased.

particles, respectively. The scattering formalism for experiments with vertically oriented $\vec{P}_{\rm B}$ and $\vec{P}_{\rm T}$ was recently described in [5]. A short summary is given in [1]. For non-identical particles, the scattered one is considered to be the same as the incident beam particle. In the $pn \to pn$ reaction, this is the outgoing proton, which could only be rescattered on the carbon analyzer. The recoil neutron spin index is absent, and we measure rescattering observables with other subscripts than those for $pp \to pp$. The fundamental laws are isospin and time-reversal invariance, and parity conservation. They relate pn with free np observables. Contrary to the case of $pp \to pp$, no symmetry conditions for pn and np observables with respect to $\theta_{\rm CM} = 90^\circ$ exist.

2 Existing elastic and quasi-elastic data

We give a list of the previously existing pn and np data measured between 1.0 and 2.7 GeV, which can be compared with the present results.

The np measurements within the nucleon–nucleon program at SATURNE II using free polarized neutrons gave 11 np spin-dependent elastic scattering observables in the interval $0.84 \leq T_{\rm kin} \leq 1.10$ GeV and the total cross section differences $\Delta\sigma_{\rm L,T}$. These data allowed the direct reconstruction of the scattering matrix at five energies, and the results are listed in [6].

The SATURNE II elastic $A_{\rm oono}$ and $A_{\rm ooon}$ data from 1.0 to 1.1 GeV are reported in [7]. A few Saclay $A_{\rm oono}$ points up to 1.0 GeV were measured with polarized deuterons, considered as a quasi-free beam of neutrons and protons [8]. In other laboratories, in the energy region under discussion, three sets of analyzing power data were determined. They were measured with free unpolarized neutron beams with a very large energy spread. Data were obtained at the LBL BEVATRON at (1.731 ± 0.468) GeV and (2.684 ± 0.483) GeV [9] and at the ANL-ZGS at (2.205 ± 0.954) GeV [10]. The $A_{\rm oono}(pn)$ results obtained with polarized protons scattered by an unpolarized deuterium target were measured at the ANL-ZGS at 1.030 GeV [11], at 1.271 GeV [13], and at 2.205 GeV [12,13]. Other $A_{\rm ooon}(pn)$ results using an unpolarized proton beam and a polarized deuterized aliphatic alcohol target were obtained at 1.109 GeV in KEK [14].

Spin correlation $A_{\rm oonn}$ data are given in [15], and $D_{\rm onon}$ data in [16] up to 1.1 GeV. Above this energy two $A_{\rm oonn}$ data points were measured with the 6 GeV/c free polarized neutron beam produced by 12 GeV/c polarized deuterons from the ANL-ZGS [17]. Otherwise, only the spin-dependent total cross differences $\Delta\sigma_L$ were determined. One set was deduced from ANL-ZGS pd and pp measurements [18]. Another one was measured with free neutrons at the JINR Synchrophasotron [19].

The existing data, including total cross sections and a few sets of differential cross sections, are insufficient for any conclusive PSA above 1.1 GeV.

3 Experimental setup and off-line analysis

As explained in [1], for purposes of the present experiment, two new target containers for the Saclay frozen spin polarized target [20] were constructed. They were inserted in the same refrigerator. One of them contained ^{6}LiD and the second ^{6}LiH irradiated materials. The targets were polarized in a homogeneous magnetic field of 2.5 Tesla. This arrangement allowed both targets to be polarized and inserted in the beam without the cryostat being opened.

The present measurements were carried out using the nucleon–nucleon experimental setup. This apparatus is described in detail in [21]. It consists of a two-arm spectrometer with an analyzing magnet and a neutron counter (NC) hodoscope in the arm on the right-hand side (RS). The NC hodoscope was made from 15 horizontal scintillation bars 300 cm long, 8 cm high, and 20 cm wide. The two photomultipliers at each end allowed the measurement of the particle position from the difference of the light propagation time. For the neutron detection, the NC was protected by four large veto counters. Either one or two contiguous NC counters only were accepted for the events. The detection efficiency of the NC was about 20%.

On the left-hand side (LS) arm, a 6-cm-thick carbon plate was positioned. Each arm was equipped with single scintillation counters and counter hodoscopes. The counter signals, including those of the NC hodoscope, triggered eight multiwire proportional chambers (MWPC) with three wire planes each. Three different triggers were simultaneously used:

1. pp trigger: An outgoing charged particle was detected by counter signals in each arm.
2. pnR trigger: A neutral particle was detected by the NC hodoscope in the RS arm, and a charged particle was seen in the conjugate arm.
3. pnL trigger: A charged particle in the RS arm was detected by scintillation counters including the NC hodoscope, and analyzed by the magnet. A neutral particle in the LS arm was converted into a charged particle in the carbon plate. The conversion efficiency was $\sim 2\%$.

The scintillation counters also measured time of flight (TOF). For the pnR trigger, no magnetic analysis existed, and the TOF measurement was crucial. The "start" signal was defined by the outgoing proton. The "stop" signal was always provided by the NC hodoscope.

Some of the charged particles in the LS arm rescattered on the carbon plate used as a polarization analyzer. The azimuthal angle distribution was measured by the MWPC.

The acceptance of each arm in the laboratory frame was $\sim \pm 4.5^\circ$ vertically and 23° horizontally. The ϕ acceptance of both arms together was limited to $\pm 8^\circ$. A complete tracking for each recorded event was performed. This is described in detail in [5,21].

There is an important difference between the elastic scattering of free neutrons on target protons and quasi-elastic scattering of protons on target nuclei. In the first case, np events were well selected by the hydrogen peak

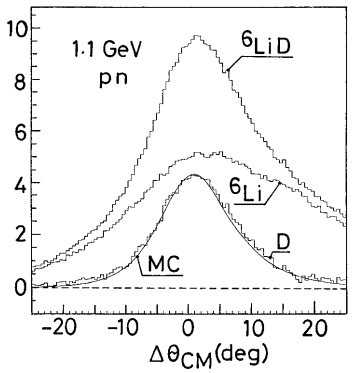

Fig. 1. The $\Delta\theta_{\rm CM}$ distribution at 1.095 GeV for events from *pn* scattering on ^{6}Li+D in the ^{6}LiD target is plotted together with that on ^{6}Li in ^{6}LiH. The normalized subtraction of numbers of events from both targets gives the distribution for deuterons. It is compared with that calculated by a Monte Carlo simulation (MC). All distributions are in arbitrary units

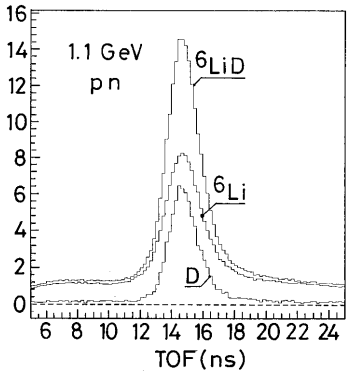

Fig. 2. The TOF spectrum at 1.095 GeV (arbitrary units) from the same targets as in Fig. 1. The normalized difference of counts, corresponding to proton scattering on neutrons in D, is also shown

in the angular correlation $\Delta\theta_{\rm CM}$ and the coplanarity $\delta\phi$. All remaining events represent a small background. In the second case, *pp* and *pn* quasi-elastic scattering displayed broad correlations.

The $\Delta\theta_{\rm CM}$ distributions of *pn* events at 1.1 GeV are shown in Fig. 1. We compare the spectrum of events scattered on ^{6}LiD and on ^{6}Li in ^{6}LiH. The normalized difference of counts, corresponding to proton scattering on neutrons in D, is also shown. In addition, the Monte Carlo simulation, based on the Hulthen distribution of the Fermi motion [1], is compared with the spectrum obtained for pure deuterons. One can see a good agreement of the simulation with the measurements. As a first selection of events, we applied a cut in the plane $\Delta\theta_{\rm CM}$ and $\Delta\phi$, represented by an ellipse with the axes of $[-10°, +12°]$ and $[-12°, +12°]$, respectively.

For the selected events, the *pn* TOF distribution at 1.1 GeV is shown in Fig. 2. In contrast to the *pp* TOF spectrum, which gave a very clean peak and very small background, the distribution for *pn*R triggers shows a very large background contamination. This is due in part to the reactions $pp \to np\pi^+$, where the p or the π goes unseen. The comparison among the TOF distributions obtained

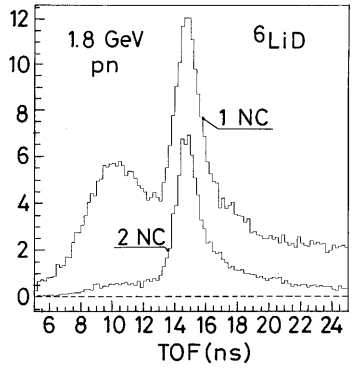

Fig. 3. The TOF spectra at 1.795 GeV recorded with either one or two adjacent neutron counter (NC) signals. Since TOF are corrected for *pn* elastic kinematics to get values independent on $\theta_{\rm CM}$, the prompt γ signals appear as a broad peak on the left

for ^{6}LiH, ^{6}LiD, and CH_2, respectively, showed that the background increased strongly with the atomic number of the target nucleus. This suggests that a large contribution to the background is due either to inelastic processes in the nuclear matter or to the spectator part of the nucleus, which disintegrates liberating gammas or low-speed neutrons. On the other hand, fast neutral particles were observed by TOF. They were clearly identified as prompt gammas mainly due to decay of π° from inelastic reactions. At 1.6 GeV, the γ peak could still be separated from normal (quasi-)elastic events. The selection became more difficult as energy increased, since the background is more important, and the prompt-γ peak is closer to *pn* quasi-elastic scattering.

However, we observed that events with two hit neutron counters (about one third of the events) displayed less important background, as shown in Fig. 3. We can explain this effect: the photons in the energy interval 0.01 to 1.0 GeV have a free mean path between 30 and 55 cm, and 50% and 30% of them, respectively, are absorbed in the scintillator. The most probable symmetric angle between e^- and e^+ at $T_\gamma = 0.1$ GeV is $\alpha = 1.5°$; the mean multiple scattering angle of the 0.05 GeV electron is $\delta = 10.5°$, and its absorption length is d = 20 cm in the scintillator. For $T_\gamma = 1$ GeV, we have $\alpha = 0.21°$ and $\delta = 0.52°$. The (e^-, e^+) pairs in NC from gammas below 1 GeV are more collimated than the charge-exchange processes used for the neutron detection, and thus γ are less susceptible to being seen in two joint NC. We have used this property to separate events in two sets with very different backgrounds. At the highest energy (2.4 GeV), the ^{6}Li TOF spectrum from a one-NC trigger (1-NC) contained $\sim 75\%$ of background. This contamination was only $\sim 32\%$ for two-NC (2-NC) triggers.

The absolute asymmetry, calculated at different TOF values, went through a maximum at the kinematic peak and dropped rapidly on both sides of this peak. The contamination by the background was estimated and subtracted using the off-peak ^{6}Li and ^{6}LiD events. Nevertheless, there remains some uncertainty concerning the real shape of the background under the peak.

Table 1. The *pn* analyzing power A_{oono} of polarized protons scattered on the polarized and/or unpolarized ^{6}LiD and ^{6}LiH targets. The first sets of results were obtained through the use of the forward outgoing protons and neutron charge- exchange in the carbon analyzer. The second sets were obtained with protons scattered at large angles and correlated neutrons detected in the NC hodoscope. The results for neutrons scattered on *D* were also deduced at 1.095 GeV. They are dependent on the data measured with both targets. Quoted errors are statistical uncertainties. The relative normalization systematic error in the beam polarization was ±3%

	$T_{\mathrm{kin}} = 1.095$ GeV,		$p_{\ell\mathrm{ab}} = 1.804$ GeV/c	
θ_{CM}	$-t$	$A_{\mathrm{oono}}(pn)$	$A_{\mathrm{oono}}(pn)$	$A_{\mathrm{oono}}(pn)$
(deg)	$(\mathrm{GeV/c})^2$	$^6\mathrm{Li} + \mathrm{D}$	D	^{6}Li
54.2	0.427	$+0.262 \pm 0.076$		
56.7	0.464		$+0.150 \pm 0.076$	$+0.224 \pm 0.039$
57.3	0.473	$+0.173 \pm 0.034$		
61.0	0.531	$+0.180 \pm 0.026$	$+0.180 \pm 0.074$	$+0.160 \pm 0.034$
65.0	0.593	$+0.098 \pm 0.026$	$+0.111 \pm 0.069$	$+0.092 \pm 0.033$
69.0	0.660	$+0.057 \pm 0.027$	$+0.118 \pm 0.080$	$+0.036 \pm 0.035$
73.0	0.727	-0.003 ± 0.029	-0.031 ± 0.080	$+0.004 \pm 0.037$
76.9	0.795	-0.043 ± 0.034	$+0.012 \pm 0.083$	-0.073 ± 0.044
80.9	0.866	-0.095 ± 0.043	$+0.008 \pm 0.100$	-0.149 ± 0.056
84.9	0.938	-0.207 ± 0.046	-0.244 ± 0.109	-0.150 ± 0.061
89.6	1.021	-0.271 ± 0.044	-0.279 ± 0.097	-0.240 ± 0.058
83.4	0.911	-0.236 ± 0.020	-0.249 ± 0.040	-0.179 ± 0.032
87.1	0.977	-0.283 ± 0.014	-0.287 ± 0.031	-0.223 ± 0.021
91.0	1.046	-0.297 ± 0.014	-0.322 ± 0.029	-0.255 ± 0.021
95.0	1.118	-0.279 ± 0.014	-0.347 ± 0.032	-0.262 ± 0.019
99.0	1.190	-0.290 ± 0.014	-0.265 ± 0.029	-0.268 ± 0.019
103.0	1.260	-0.263 ± 0.013	-0.301 ± 0.029	-0.238 ± 0.019
107.0	1.329	-0.259 ± 0.013	-0.255 ± 0.030	-0.250 ± 0.019
111.0	1.397	-0.254 ± 0.013	-0.294 ± 0.031	-0.232 ± 0.018
115.0	1.464	-0.258 ± 0.013	-0.224 ± 0.030	-0.240 ± 0.018
119.0	1.527	-0.222 ± 0.013	-0.206 ± 0.028	-0.228 ± 0.019
123.0	1.589	-0.240 ± 0.014	-0.268 ± 0.029	-0.227 ± 0.020
126.8	1.645	-0.199 ± 0.015	-0.149 ± 0.032	-0.196 ± 0.023
130.0	1.690	-0.148 ± 0.034	-0.216 ± 0.057	-0.062 ± 0.052

The pure deuteron asymmetry was obtained by subtraction of the number of selected events for the ^{6}Li and the ^{6}LiD measurements. These counts were normalized by the beam intensity and the effective target densities. The normalization may introduce an additional absolute uncertainty on the order of ±0.04 for $A_{\mathrm{oono}}(np)$. The TOF distribution for *D* shows a very small background (see Fig. 2), which was not subtracted.

The cuts for single scattering changed the relative trigger contributions from the target components. For *pn*R events at 1.1 GeV with ^{6}LiD, we had 54% of the effective triggers from ^{6}Li and 46% from D. For *pn*L, these amounts were 59% from ^{6}Li, and 41% from D.

From the set of the selected single scattering events, we kept events where the proton rescattered in the carbon analyzer at $\theta_C \geq 4°$. This second scattering selection procedure is described in [5], where an exhaustive list of relevant references for the $p - C$ analyzing power is given. The proton–carbon scattering, with one outgoing charged particle, introduces a relative systematic error of ±6% for any rescattering observable at any energy. The resulting angular dependence of D_{nono} was determined using the method first proposed by the Geneva group [22].

The triggers for *pn* events on C in the CH_2 target, downstream from the main target, were independent from those used for the polarized target. Events were recorded by the same apparatus and analyzed using identical criteria for single scattering [1].

Table 1. (continued)

$T_{\rm kin} = 1.595$ GeV, $p_{\ell\rm ab} = 2.353$ GeV/c			$T_{\rm kin} = 1.795$ GeV, $p_{\ell\rm ab} = 2.567$ GeV/c		
$\theta_{\rm CM}$ (deg)	$-t$ (GeV/c)^2	$A_{\rm oono}(pn)$ ^{6}Li + D	$\theta_{\rm CM}$ (deg)	$-t$ (GeV/c)^2	$A_{\rm oono}(pn)$ ^{6}Li + D
66.6	0.902	-0.022 ± 0.093	71.3	1.145	$+0.044 \pm 0.068$
73.8	1.081	-0.077 ± 0.054	84.0	1.510	-0.061 ± 0.073
84.7	1.360	-0.174 ± 0.050	– – – – – – – – – – – – – – – – – –		
– – – – – – – – – – – – – – – – – –			72.5	1.180	-0.141 ± 0.067
77.7	1.178	-0.096 ± 0.022	78.1	1.338	-0.134 ± 0.032
85.0	1.369	-0.161 ± 0.020	86.0	1.569	-0.178 ± 0.036
93.1	1.579	-0.107 ± 0.019	94.1	1.806	-0.151 ± 0.038
101.1	1.787	-0.176 ± 0.019	102.1	2.040	-0.111 ± 0.037
109.1	1.988	-0.176 ± 0.016	110.0	2.263	-0.154 ± 0.029
116.5	2.167	-0.178 ± 0.016	116.9	2.450	-0.151 ± 0.035
$T_{\rm kin} = 1.895$ GeV, $p_{\ell\rm ab} = 2.674$ GeV/c			$T_{\rm kin} = 2.035$ GeV $p_{\ell\rm ab} = 2.822$ GeV/c		
$\theta_{\rm CM}$ (deg)	$-t$ (GeV/c)^2	$A_{\rm oono}(pn)$ ^{6}Li + D	$\theta_{\rm CM}$	$-t$	$A_{\rm oono}(pn)$
71.5	1.216	-0.061 ± 0.066	71.0	1.291	-0.200 ± 0.069
83.7	1.584	-0.108 ± 0.072	82.7	1.669	-0.112 ± 0.086
– – – – – – – – – – – – – – – – – –			– – – – – – – – – – – – – – – – – –		
72.5	1.246	-0.016 ± 0.074	72.6	1.340	-0.092 ± 0.077
78.1	1.413	-0.136 ± 0.040	78.2	1.520	-0.152 ± 0.037
86.0	1.657	-0.168 ± 0.049	86.1	1.782	-0.106 ± 0.048
94.1	1.907	-0.168 ± 0.056	94.0	2.045	-0.138 ± 0.056
102.1	2.153	-0.201 ± 0.048	102.1	2.312	-0.160 ± 0.052
110.0	2.389	-0.080 ± 0.038	110.1	2.569	-0.094 ± 0.036
117.2	2.594	-0.111 ± 0.041	117.2	2.786	-0.076 ± 0.039

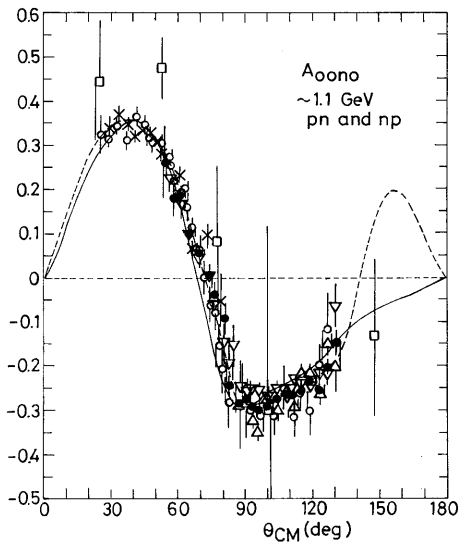

Fig. 4. The $A_{\rm oono}$ results at 1.095 GeV. •: protons scattered on ^{6}Li + D neutrons in the ^{6}LiD target; ▽: *pn* on ^{6}Li in the ^{6}LiH target; △: *pn* on *D* in ^{6}LiD target; ○: see [7]; ×: 1.03 GeV ANL [10]; open squares: 1.109 GeV KEK [14]; solid curve: VPI-PSA [2]; dashed curve: SG-PSA [3]

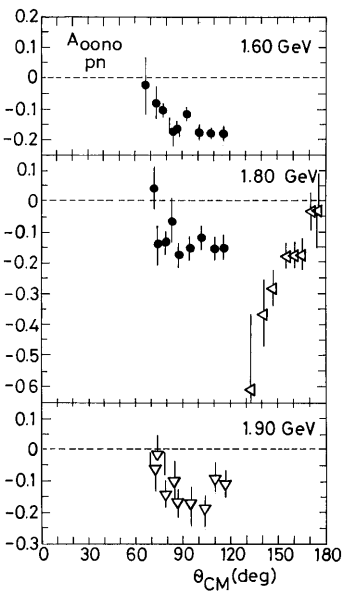

Fig. 5. $A_{\rm oono}$ results at 1.595, 1.795, and 1.895 GeV. •: protons scattered on ^{6}Li + D neutrons in the ^{6}LiD target; ▽: *pn* on ^{6}Li in the ^{6}LiH target; ◁: *np* at 1.731 GeV LBL [9]

Table 1. (continued)

$T_{\rm kin} = 2.095$ GeV, $p_{\ell\rm ab} = 2.885$ GeV/c			
$\theta_{\rm CM}$ (deg)	$-t$ (GeV/c)^2	$A_{\rm oono}(pn)$ ^{6}Li + D	$A_{\rm oono}(pn)$ ^{6}Li
71.2	1.335	-0.062 ± 0.058	$+0.008 \pm 0.091$
82.9	1.726	-0.044 ± 0.076	-0.171 ± 0.130
72.6	1.380	-0.253 ± 0.061	-0.098 ± 0.114
78.1	1.564	-0.154 ± 0.033	-0.140 ± 0.053
85.9	1.829	-0.191 ± 0.043	-0.157 ± 0.068
94.0	2.107	-0.249 ± 0.052	-0.120 ± 0.087
102.0	2.378	-0.204 ± 0.054	-0.199 ± 0.081
110.1	2.646	-0.106 ± 0.040	-0.120 ± 0.067
117.4	2.873	-0.156 ± 0.038	-0.121 ± 0.063

Table 1. (continued)

$T_{\rm kin} = 2.395$ GeV, $p_{\ell\rm ab} = 3.199$ GeV/c		
$\theta_{\rm CM}$ (deg)	$-t$ (GeV/c)^2	$A_{\rm oono}(pn)$ ^{6}Li (+D)
70.7	1.504	-0.032 ± 0.058
82.0	1.934	$+0.031 \pm 0.089$
78.4	1.797	-0.160 ± 0.042
86.1	2.098	-0.179 ± 0.055
94.0	2.409	-0.022 ± 0.066
102.0	2.719	-0.136 ± 0.063
110.0	3.021	-0.116 ± 0.045
117.4	3.287	-0.057 ± 0.040

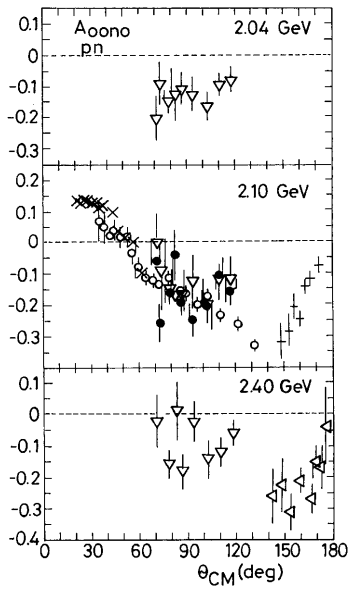

Fig. 6. $A_{\rm oono}$ results at 2.035, 2.095 and 2.395 GeV. •: protons scattered on ^{6}Li + D neutrons in the ^{6}LiD target; ▽: *pn* on ^{6}Li in the ^{6}LiH target; +: *np* at 2.205 GeV ANL [10]; ×: 2.205 GeV ANL [12]; ○: 2.205 GeV ANL [13]; ◁: *np* at 2.684 GeV LBL [9]

Table 2. The *pn* analyzing power $A_{\rm oono}$ of polarized protons scattered on neutrons bound in carbon nuclei of the CH_2 target. The meaning of the two data sets is the same as in Table 1. Quoted errors are statistical only. The relative normalization systematic error in the beam polarization was ±3%

$T_{\rm kin} = 1.091$ GeV, $p_{\ell\rm ab} = 1.800$ GeV/c		
$\theta_{\rm CM}$ (deg)	$-t$ (GeV/c)^2	$A_{\rm oono}(pn)$ C
60.4	0.518	$+0.118 \pm 0.101$
66.1	0.609	$+0.152 \pm 0.037$
73.4	0.731	$+0.036 \pm 0.051$
82.0	0.881	$+0.006 \pm 0.059$
88.1	0.990	$+0.008 \pm 0.100$
98.2	1.170	-0.278 ± 0.105
102.1	1.238	-0.344 ± 0.069
106.1	1.308	-0.209 ± 0.065
110.1	1.375	-0.199 ± 0.051
114.0	1.440	-0.274 ± 0.048
118.0	1.504	-0.179 ± 0.045
122.0	1.566	-0.314 ± 0.053
125.9	1.624	-0.155 ± 0.058
130.3	1.690	-0.256 ± 0.054

4 Results and discussion

Only the *pn* results obtained with protons scattered on the entire ^{6}LiD target and on the pure ^{6}Li in the ^{6}LiH target are completely independent. Listed energies correspond to the target centers. Errors on experimental values in the tables are statistical only. Normalization and systematic errors are mentioned.

In Table 1 are listed the $A_{\rm oono}(pn)$ data measured at all energies. At each energy, two sets are given. The results at small angles were obtained using *pn*L-triggers with an outgoing proton and a neutron charge-exchange in the carbon plate. The statistical errors of these data sets are large, but the results contain a small background contamination. The second sets were obtained using the *pn*R-triggers, with protons scattered at large angles and correlated neutrons detected in the NC hodoscope.

At 1.095 GeV, the independent results obtained in *pn* scattering on $^6Li + D$ in the ^{6}LiD and on ^{6}Li in the ^{6}LiH targets are given together with the results deduced for proton scattering on neutrons in D. At 1.595 GeV, only the ^{6}LiD target was used. At 1.795 GeV the *np* statistics for the ^{6}LiH target was poor, and the results were omitted. At 1.895, 2.035, and 2.395 GeV, the small amounts of ^{6}LiD events were added to the ^{6}Li data ($10 - -20\%$), whereas the separate statistics for both targets were used at 2.095 GeV.

All the data at 1.095 GeV are plotted in Fig. 4, along with the previous Saclay results from [7] and results from ANL-ZGS at 1.030 GeV [11] and from KEK [14]. The present data were included in the SG-PSA, but are absent

Table 3. The *pn* spin-correlation parameter A_{oonn} of polarized protons scattered on polarized neutrons bound in the ^{6}LiD target. Quoted errors are statistical uncertainties. The relative normalization systematic error in the beam polarization was ±3%, and that of the target polarization was ±4% at 1.095 GeV, and ±10% at 1.595 GeV

	$T_{kin} = 1.095$ GeV, $p_{\ell ab} = 1.804$ GeV/c			$T_{kin} = 1.595$ GeV, $p_{\ell ab} = 2.353$ GeV/c	
θ_{CM} (deg)	$-t$ $(GeV/c)^2$	$A_{oonn}(pn)$ ^{6}Li + D	θ_{CM} (deg)	$-t$ $(GeV/c)^2$	$A_{oonn}(pn)$ ^{6}Li + D
83.4	0.911	-0.132 ± 0.304	81.9	1.286	-0.320 ± 0.173
89.3	1.013	-0.224 ± 0.149	97.2	1.687	$+0.218 \pm 0.157$
97.0	1.155	-0.242 ± 0.145	112.4	2.069	$+0.274 \pm 0.135$
105.0	1.295	-0.143 ± 0.139			
113.0	1.431	-0.294 ± 0.138			
120.9	1.558	-0.362 ± 0.141			
127.4	1.654	-0.004 ± 0.213			

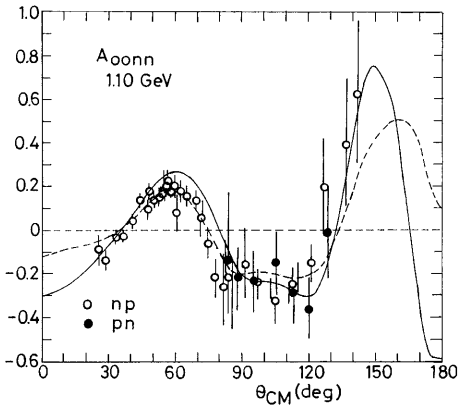

Fig. 7. A_{oonn} results at 1.095 GeV. •: protons scattered on ^{6}Li + D neutrons in the ^{6}LiD target; ○: *np* results from [15] at 1.10 GeV. Curves are as in Fig. 3

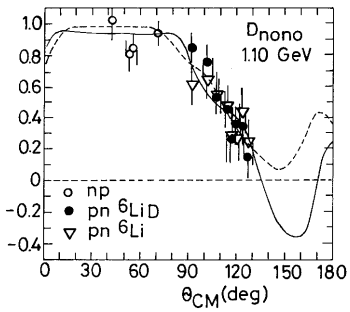

Fig. 8. $D_{nono}(pn)$ results at 1.095 GeV measured with ^{6}LiD (•) and ^{6}LiH (▽) targets, compared with the data from [16] (○). Curves are as in Fig. 4

in the VPI-PSA. The data obtained with the ^{6}LiD target need no multiplicative normalizing factor with respect to the previous Saclay results [7]. The ^{6}Li data need to be renormalized upwards by a factor of 1.09. In the angular region covered by the data, both PSA agree well. They differ for $\theta_{CM} > 140°$, as was previously observed when the new data were not introduced in the SG-PSA [3].

Our $A_{oono}(pn)$ results from 1.595 GeV to 2.395 GeV are plotted in Figs. 5 and 6. We observe that the zero-crossing point slowly moves from $\theta_{CM} \sim 73°$ at 1.1 GeV towards smaller angles at higher energies. The present results are compared with existing data.

Note that the results from other laboratories, obtained up to high energies (e.g., from [9,10,12,13]), showed that the maximum of the A_{oono} angular dependence in the forward hemisphere decreases with increasing energy, whereas the minimum analyzing power value reaches large negative values.

In Table 2 are given the quasi-elastic data obtained at 1.091 GeV with protons scattered on neutrons in carbon using the CH_2 target. The data have larger errors, but the SG-PSA fit shows that their multiplicative normalizing factor is 1.00. At other energies, the number of carbon events was small and contained a large background.

The A_{oonn} data at 1.095 and 1.595 GeV are listed in Table 3. The statistics are sufficient only for neutrons detected by the NC hodoscope (*pn*R triggers). The same is valid for the rescattering data. The A_{oonn} results at 1.095 GeV are plotted in Fig. 7. We see an excellent agreement with previous data [15] and with the PSA predictions. The data at 1.595 GeV (not plotted) suggest that the zero-crossing point in the backward hemisphere moves toward smaller angles with increasing energy.

Our $D_{nono}(pn)$ results are listed in Table 4. At 1.095 GeV, the data are plotted in Fig. 8. They were measured in the region $91° \leq \theta_{CM} \leq 127°$, where a rapid decrease of the angular dependence occurs. Data are in excellent agreement with PSA predictions in this very sensitive region. The previous SATURNE II *np* data at the same energy [16] were measured in the forward hemisphere, where the $D_{nono} = D_{onon}$ values are large and fairly constant.

5 Conclusions

Our new quasi-elastic *np* results for protons scattered on weakly bound neutrons in deuterons and in ^{6}Li nuclei

Table 4. The observable $D_{\rm nono}(pn)$ for quasi-elastic scattering of polarized protons on the ^{6}LiD and ^{6}LiH targets. The relative normalization systematic error in the beam polarization was ±3%. The relative systematic error provided by the normalization uncertainty in the p-C analyzing power was ±6%

$\theta_{\rm CM}$ (deg)	Interval (CM deg)	$-t$ (mean) (GeV/c)^2	$D_{\rm nono}(pn)$ ^{6}Li + D	$D_{\rm nono}(pn)$ ^{6}Li
	$T_{\rm kin}$ = 1.095 GeV,		$p_{\ell\rm ab}$ = 1.804 GeV/c	
91.3	81.1–98.0	1.051	$+0.848 \pm 0.092$	$+0.584 \pm 0.118$
101.7	98.0–105.0	1.236	$+0.752 \pm 0.107$	$+0.644 \pm 0.134$
107.4	105.0–110.0	1.335	$+0.541 \pm 0.117$	$+0.562 \pm 0.143$
112.0	110.0–114.0	1.412	$+0.483 \pm 0.122$	$+0.495 \pm 0.143$
115.5	114.0–117.0	1.470	$+0.250 \pm 0.133$	$+0.263 \pm 0.159$
119.0	117.0–121.0	1.525	$+0.366 \pm 0.114$	$+0.239 \pm 0.138$
122.6	121.0–124.0	1.581	$+0.354 \pm 0.122$	$+0.457 \pm 0.157$
126.7	124.0–131.1	1.641	$+0.140 \pm 0.123$	$+0.249 \pm 0.154$
	$T_{\rm kin}$ = 1.595 GeV,		$p_{\ell\rm ab}$ = 2.353 GeV/c	
88.0	72.5–100.0	1.444	$+0.601 \pm 0.114$	
105.1	100.0–110.0	1.756	$+0.489 \pm 0.143$	
114.3	110.0–122.6	2.112	$+0.463 \pm 0.134$	
	$T_{\rm kin}$ = 1.795 GeV,		$p_{\ell\rm ab}$ = 2.567 GeV/c	
88.0	71.0–104.0	1.625	$+0.302 \pm 0.218$	
110.1	104.0–110.0	2.263	$+0.242 \pm 0.276$	
	$T_{\rm kin}$ = 1.895 GeV,		$p_{\ell\rm ab}$ = 2.674 GeV/c	
89.3	72.0–104.0	1.756		$+0.839 \pm 0.268$
110.9	104.0–120.0	2.412		$+0.185 \pm 0.327$
	$T_{\rm kin}$ = 2.035 GeV,		$p_{\ell\rm ab}$ = 2.822 GeV/c	
89.3	71.0–104.0	1.886		$+0.779 \pm 0.262$
111.4	104.0–121.0	2.606		-0.152 ± 0.330
	$T_{\rm kin}$ = 2.095 GeV,		$p_{\ell\rm ab}$ = 2.885 GeV/c	
88.9	70.0–104.0	1.928	$+0.642 \pm 0.215$	
111.2	104.0–120.0	2.676	$+0.702 \pm 0.263$	
	$T_{\rm kin}$ = 2.395 GeV,		$p_{\ell\rm ab}$ = 3.199 GeV/c	
89.9	72.0–104.0	2,243		$+0.058 \pm 0.241$
111.4	104.0–120.0	3.067		-0.102 ± 0.260

show good agreement with *np* elastic scattering data. The present comparison of elastic and quasi-elastic scattering results suggests that an ^{6}LiD target, polarized deuteron jet, or polarized deuteron beam may be successfully used for *pn* spin-dependent experiments. Above 1.5 GeV, accurate multiple TOF measurements are needed, or they must be complemented by a magnetic analysis of the singly scattered protons. A discrimination between the signals from neutrons and those from γ rays in the NC hodoscope may be also useful. In our case, a more segmented NC hodoscope would be more selective against γ. As in the preceding paper, the data suggest that no additional corrections to the raw data are needed. The quasi-elastic $A_{\rm oono}(pn)$ data on strongly bound nucleons in carbon nuclei are in good agreement, but they are more affected by inelastic reactions.

The present *pn* results at 1.095 GeV improve significantly the existing spin-dependent database and constrain the PSA in a sensitive angular region. Above the maximum neutron energy accessible at SATURNE II, the $D_{\rm nono}$ data represent the first measurements ever. Nevertheless, the possibility to perform *np* PSA above 1.1 GeV remains uncertain, and new independent data are highly desirable.

Acknowledgements. We thank C. Lechanoine-Leluc for her help with the new SG-PSA results. We express our gratitude to R.A. Arndt and I.I. Strakovsky for providing us the very recent VPI-PSA predictions (SAID-SP99). This work was supported in part by the U.S. Department of Energy, Division of Nuclear Physics, Contract No. W-31-109-ENG-38, by the Swiss National Science Foundation, and by the Russian Foundation for Fundamental Nuclear Physics Programme 122.03.

References

1. J. Ball, C.E. Allgower, M. Beddo, J. Bystrický, M. Combet, Ph. Demierre, G. Durand, J.-M. Fontaine, D. Grosnick, R. Hess, Z. Janout, Z.F. Janout, V.A. Kalinnikov, T.E. Kasprzyk, B.A. Khachaturov, R. Kunne, F. Lehar, A. de Lesquen, D. Lopiano, V.N. Matafonov, I.L. Pisarev, A.A. Popov, A.N. Prokofiev, D. Rapin, J.-L. Sans, H.M. Spinka, Yu.A. Usov, V.V. Vikhrov, B. Vuaridel, and A.A. Zhdanov, Eur. Phys. J. C, preceding paper
2. R.A. Arndt, C.H. Oh, I.I. Strakovsky, R.L. Workman, and F. Dohrman, Phys. Rev. **C56**, 3005 (1997); SAID solution SP99
3. J. Ball, J. Bystrický, J.-M. Fontaine, G. Gaillard, R. Hess, Z. Janout, B.A. Khachaturov, R. Kunne, C.D. Lac, C. Lechanoine-Leluc, F. Lehar, A. de Lesquen, D. Lopiano, F. Perrot-Kunne, D. Rapin, L. van Rossum, H. Schmitt, and H.M. Spinka, Nuovo Cimento **A111**, 13 (1998)
4. J. Bystrický, F. Lehar, and P. Winternitz, J. Physique (Paris) **39**, 1 (1978)
5. C.E. Allgower, J. Ball, L.S. Barabash, M. Beddo, Y. Bedfer, A. Boutefnouchet, J. Bystrický, P.-A. Chamouard, Ph. Demierre, J.-M. Fontaine, V. Ghazikhanian, D. Grosnick, R. Hess, Z. Janout, Z.F. Janout, V.A. Kalinnikov, T.E. Kasprzyk, Yu.M. Kazarinov, B.A. Khachaturov, R. Kunne, C. Lechanoine-LeLuc, F. Lehar, A. de Lesquen, D. Lopiano, M. de Mali, V.N. Matafonov, I.L. Pisarev, A.A. Popov, A.N. Prokofiev, D. Rapin, J.-L. Sans, H.M. Spinka, Yu.A. Usov, V.V. Vikhrov, B. Vuaridel, C.A. Whitten, and A.A. Zhdanov, Eur. Phys. J. C **5**, 453 (1998)
6. D. Adams, J. Arvieux, H. Azaiez, P. Bach, J. Ball, L.S. Barabash, R. Binz, J. Bystricky, P. Chaumette, Ph. Demierre, J. Derégel, J.M. Fontaine, G. Gaillard, V. Ghazikhanian, J. Gordon, T. Hasegawa, R. Hess, Z. Janout, B.A. Khachaturov, A. Klett, R. Kunne, C.D. Lac, F. Lehar, M.C. Lemaire, A. de Lesquen, D. Lopiano, M. de Mali, A. Michalowicz, C.R. Newsom, Y. Onel, A. Penzo, F. Perrot-Kunne, R. Peshina-Klett, D. Rapin, C. Raymond, E .Rössle, L. van Rossum, H. Schmitt, J.L. Sans, P. Sormani, H. Spinka, Yu.A. Usov, B. Vuaridel, and C.A. Whitten, Acta Polytechnica (Prague) **36**, 11 (1996)
7. J. Ball, Ph. Chesny, M. Combet, J.M. Fontaine, C.D. Lac, J.L. Sans, J. Bystricky, F. Lehar, A. de Lesquen, M. de Mali, F. Perrot-Kunne, L. van Rossum, A. Ahmidouch, P. Bach, Ph. Demierre, G. Gaillard, R. Hess, R. Kunne, D. Rapin, Ph. Sormani, J.P. Goudour, R. Binz, A. Klett, E. Rössle, H. Schmitt, D. Lopiano, and H. Spinka, Nucl. Phys. **A559**, 489 (1993)
8. J. Ball, V. Ghazikhanian, J. Gordon, F. Lehar, A. de Lesquen, F. Perrot, and L. van Rossum, Nucl. Phys. **B286**, 635 (1987)
9. P.R. Robrish, O. Chamberlain, R.D. Field, Jr., R.Z. Fuzesy, W. Gorn, C.C. Morehouse, T. Powell, S. Rock, S. Shannon, G. Shapiro, H. Weisberg, and M.J. Longo, Phys. Lett. **31B**, 617–620 (1970); the numerical table was obtained from P.R. Robrish in 1978
10. M.A. Abolins, M.T. Lin, R.C. Ruchti, J.G. Horowitz, R.C. Kammerud, N.W. Reay, K. Reibel, N.R. Stanton, K.W. Edwards, D.G. Crabb, and J.R. O'Fallon, Phys. Rev. Lett. **30**, 1183 (1973); the numerical table was obtained from D.G. Crabb in 1976
11. M.L. Marshak, E.A. Peterson, K. Ruddick, J. Lesikar, T. Mulera, J.B. Roberts, R.D. Klem, R. Talaga, and A. Wriekat, Phys. Rev. **C18**, 331 (1978)
12. R. Diebold, D.S. Ayres, S.L. Kramer, A.J. Pawlicki, and A.B. Wicklund, Phys. Rev. Lett. **35**, 632 (1975)
13. Y. Makdisi, M.L. Marshak, B. Mossberg, E.A. Peterson, K. Ruddick, J.B. Roberts, and R.D. Klem, Phys. Rev. Lett. **45**, 1529 (1980); the numerical values are in the thesis of Björn Mossberg from University of Minnesota
14. M. Sakuda, S. Isagawa, S. Ishimoto, S. Kabe, A. Masaike, K. Marimoto, K. Ogawa, M. Suetake, F. Takasaki, Y. Watase, N. Kim, S. Kobayashi, A. Murakami, A. de Lesquen, K. Nakajima, S. Nakada, T. Wada, and I. Yamauchi, Phys. Rev. **D25**, 2004 (1982)
15. J. Ball, Ph. Chesny, M. Combet, J.-M. Fontaine, C.D. Lac, M.C. Lemaire, J.L. Sans, J. Bystrický, F. Lehar, A. de Lesquen, M. de Mali, F. Perrot-Kunne, L. van Rossum, P. Bach, Ph. Demierre, G. Gaillard, R. Hess, R. Kunne, D. Rapin, Ph. Sormani, B. Vuaridel, J.P. Goudour, R. Binz, A. Klett, E. Rössle, H. Schmitt, L.S. Barabash, Z. Janout, B.A. Khachaturov, Yu.A. Usov, D. Lopiano, and H. Spinka, Nucl. Phys. **A559**, 511 (1993); Nucl. Phys. **A576**, 640(E) (1994)
16. J. Ball, Ph. Chesny, M. Combet, J.-M. Fontaine, R. Kunne, M.C. Lemaire, J.L. Sans, J. Bystrický, C.D. Lac, F. Lehar, A. de Lesquen, M. de Mali, F. Perrot-Kunne, L. van Rossum, P. Bach, Ph. Demierre, G. Gaillard, R. Hess, D. Rapin, Ph. Sormani, J.P. Goudour, R. Binz, A. Klett, R. Peshina-Klett, E. Rössle, H. Schmitt, L.S. Barabash, Z. Janout, B.A. Khachaturov, Yu.A. Usov, D. Lopiano, and H. Spinka, Zeitschrift für Physik **C61**, 579 (1994)
17. D.G. Crabb, P.H. Hansen, A.D. Krisch, T. Shima, K.M. Terwilliger, E.A. Crosbie, L.G. Ratner, P.F. Schultz, G.H. Thomas, J.R. O'Fallon, A. Lin, A.J. Salthouse, and A. Perlmutter, Phys. Rev. Lett. **43**, 983–986 (1979)
18. I.P. Auer, W.R. Ditzler, D. Hill, H. Spinka, N. Tamura, G. Theodosiou, K. Toshioka, D. Underwood, R. Wagner, and A.Yokosawa, Phys. Rev. Lett. **46**, 1177 (1981)
19. B.P. Adiasevich, V.G. Antonenko, S.A. Averichev, L.S. Azhgirey, J. Ball, N.A. Bazhanov, B. Benda, N.S. Borisov, Yu.T. Borzunov, E.I. Bunyatova, V.F. Burinov, E.V. Chernykh, S.A. Dolgii, G. Durand, A.P. Dzyubak, A.N. Fedorov, V.V. Fimushkin, J.M. Fontaine, V.V. Glagolev, L.B. Golovanov, D.P. Grosnick, G.M. Gurevich, D.A. Hill, A.V. Karpunin, T.E. Kasprzyk, B.A. Khachaturov, A.D. Kirillov, N.I. Kochelev, A.D. Kovalenko, A.I. Kovalev, M.V. Kulikov, V.P. Ladygin, A.B. Lazarev, F. Lehar, A. de Lesquen, M.Yu. Liburg, D. Lopiano, A.A. Lukhanin, P.K. Maniakov, V.N. Matafonov, E.A. Matyushevsky, G. Mgebrishvili, S.V. Mironov, A.B. Neganov, G.P. Nikolaevsky, A.A. Nomofilov, Yu.K. Pilipenko, I.L. Pisarev, N.M. Piskunov, Yu.A. Plis, Yu.P. Polunin, V.V. Polyakov, A.N. Prokofiev, D.A. Ronzhin, P.A. Rukoyatkin, J.L. Sans, V.I. Sharov, S.N. Shilov, Yu.A. Shishov, V.B. Shutov, P.V. Sorokin, H.M. Spinka, A.Yu. Starikov, G.D. Stoletov, E.A. Strokovsky, L.N. Strunov, A.L. Svetov, V.V. Teterin, S.V. Topalov, V.Yu. Trautman, A.P. Tsvinev, Yu.A. Usov, V.V. Vikhrov, V.I. Volkov, A.A. Yershov, V.P. Yershov, S.A. Zaporozhets, and A.A. Zhdanov, Zeitschrift für Physik **C71**, 65 (1996)
20. J. Ball, M. Combet, J.-L. Sans, B. Benda, P. Chaumette, J. Derégel, G. Durand, A.P. Dzyubak, C. Gaudron, F. Lehar, A. de Lesquen, T.E. Kasprzyk, Z. Janout, B.A. Khachaturov, V.N. Matafonov, and Yu.A. Usov, Nucl. Instrum. Methods **A381**, 4 (1996)

21. J. Ball, Ph. Chesny, M. Combet, J.-M. Fontaine, R. Kunne, J.-L. Sans, J. Bystrický, C.D. Lac, D. Legrand, F. Lehar, A. de Lesquen, M. de Mali, F. Perrot-Kunne, L. van Rossum, P. Bach, Ph. Demierre, G. Gaillard, R. Hess, Z.F. Janout, D. Rapin, Ph. Sormani, B. Vuaridel, J.P. Goudour, R. Binz, A. Klett, E. Rössle, H. Schmitt, L.S. Barabash, Z. Janout, V.A. Kalinnikov, Yu.M. Kazarinov, B.A. Khachaturov, V.N. Matafonov, I.L. Pisarev, A.A. Popov, Yu.A. Usov, M. Beddo, D. Grosnick, T. Kasprzyk, D. Lopiano, and H. Spinka, Nucl. Instrum. Methods **A327**, 308 (1993)
22. D. Besset, Q.H. Do, B. Favier, L.G. Greeniaus, R. Hess, C. Lechanoine, D. Rapin, D.W. Werren, and Ch.Weddigen, Nucl. Instrum. Methods **166**, 379 (1979)